AD-A064 803 AIR FORCE FLIGHT DYNAMICS LAB WRIGHT-PATTERSON AFB OHIO F/G 20/4
EFFECT OF BLUNTNESS AND ANGLE OF ATTACK ON BOUNDARY LAYER TRANS--ETC(U)
1978 K F STETSON

UNCLASSIFIED NL

| OF |
ADA
064803

END
DATE
FILMED
4-79
DDC

79-0269

Effect of Bluntness and Angle of Attack on Boundary Layer Transition on Cones and Biconic Configurations

K.F. Stetson, *Flight Dynamics Lab, Wright-Patterson AFB, Ohio*

Kenneth F. Stetson

17th AEROSPACE SCIENCES MEETING

New Orleans, La./January 15-17, 1979

EFFECT OF BLUNTNESS AND ANGLE OF ATTACK ON BOUNDARY LAYER TRANSITION ON CONES AND BICONIC CONFIGURATIONS

Kenneth F. Stetson *

Air Force Flight Dynamics Laboratory
Air Force Wright Aeronautical Laboratories
Wright-Patterson AFB, Ohio

ABSTRACT

New wind tunnel data has been obtained to investigate the effects of tip bluntness and angle of attack on boundary layer transition. The rearward displacement of transition due to bluntness was found to be quite sensitive to free stream Mach number as well as entropy swallowing. At M_∞=9.3 transition could be displaced rearward as much as nine times the transition length of the sharp cone. The trend of maximum transition displacement with free stream Mach number followed the trend of reduced Reynolds number. Reynolds number reduction due to pressure losses across the bow shock was believed to be the dominant effect associated with the rearward displacement of transition on a blunt cone. Transition location was sensitive to small changes in angle of attack, and both the sharp and blunt tips produced a rearward movement of transition on the windward ray at small angles of attack. No significant increase from the conical transition Reynolds numbers were found on the biconic configurations. In fact, the biconic configurations tested often had an earlier transition.

NOMENCLATURE

d	distance the model sting is off the tunnel centerline (in.)
h	local heat transfer coefficient (Btu/ft^2-sec $^\circ$R)
L	leeward side
M	Mach number
p	surface pressure (used in nondimensional ratio)
$\dot{q}$	heat transfer rate (used in nondimensional ratio)
R	model nose or base radius (in.)
Re	Reynolds number
Re_Θ	Reynolds number based upon conditions at the edge of the boundary layer and momentum thickness
Re_{x_T}	transition Reynolds number based upon conditions at the edge of the boundary layer and surface distance from the sharp tip or stagnation point to the location of transition.
X or S	surface distance (in.)
X_{sw}	swallowing distance (see Fig. 7) (in.)
X_T	distance from the sharp tip or stagnation point to the onset of transition (An exception is Fig. 1-Pate's predictions are based upon the end of transition) (in.)
X_{T_B} or $(X_T)_B$	distance to onset of transition on blunt configurations (in.)
X_{T_s} or $(X_T)_s$	distance to onset of transition on sharp configurations (in.)
W	windward
α	angle of attack (degrees)
Θ_c	cone half angle (degrees)

SUBSCRIPTS

B	base or blunt
N	nose
ST	model stagnation point
∞	free stream

INTRODUCTION

Boundary layer transition is a problem that has plagued several generations of aerodynamicists. Although significant advances in stability theory and turbulence modeling have been made in recent years (e.g. Mack[1], Wilcox[2]), the technology in this area has lagged far behind most other aerodynamic areas. The development of the theory has been slow because of the extreme complexity of the problem and understanding through experimentation has been hampered by the difficulty of conducting a "good" experiment. The wind tunnel, which has been the major source of experimental aerodynamic data, has provided a vast amount of transition data; yet the majority of these data have produced empirical correlations which have not added a great deal to the general understanding of transition phenomena. In recent years it has been generally accepted that wind tunnel disturbances can dominate transition results (e.g. Pate[3]) and that transition Reynolds numbers obtained in wind tunnels should not be related directly to flight situations. In spite of this short-coming of wind tunnel testing, it may be possible to obtain valid transition trends from "noisy" wind tunnel experiments. The approach of this present investigation was to explore some of the hypersonic features of bluntness and angle of attack transition trends. The hypersonic wind tunnels used, as all current hypersonic wind tunnels, were "noisy" wind tunnels as a result of aerodynamic noise generated by the turbulent boundary layer on the nozzle wall.

* Aerospace Engineer, High Speed Aero Performance Branch, Aeromechanics Division: Associate Fellow AIAA

Paper #79-0267

A check was made of the generality of the transition trends by comparing these present data with data from other facilities and by obtaining transition data off the tunnel centerline. Although the results obtained appeared to be consistent and valid, these data, as all wind tunnel transition data, should be treated with caution until more knowledge of transition phenomena is available.

EXPERIMENTAL APPARATUS AND PROCEDURES

The experiments were conducted in the AFFDL Mach 6 wind tunnel and the AEDC Tunnel F.

The Mach 6 tunnel is a blow-down facility operating at a reservoir temperature near 1100°R and a reservoir pressure range of 700 to 2100 psia, corresponding to a Reynolds number per foot range of 9.7×10^6 to 30.3×10^6. The test core is produced by a contoured axisymmetric nozzle with an exit diameter of 12.3 inches. Additional details of the tunnel can be found in Ref. 4. The test model for the Mach 6 tunnel was a thin-skin (nominally 0.025 inches), 8-degree half angle cone containing two rays of thermocouples, located 180 degrees apart. The base diameter of the model was 4 inches and the model had nosetips with the following bluntness ratios; R_N/R_B = 0, 0.02, 0.05, 0.10, 0.15, and 0.30. Nominal model surface finish was 15 microinches and the blunt nose tips were polished before each run. A 14-degree half angle cone section was added to the front portion of the 8-degree cone to obtain data on a biconic configuration. The junction of the two cones was at a station 35% of the sharp 8-degree cone length. Two tip configurations were tested; sharp and 7.4% of the base radius (21% of the base of the 14-degree cone).

The AEDC Tunnel F is an arc-driven wind tunnel of the hotshot type and capable of providing Mach numbers from about 7 to 13 over a Reynolds number per foot range from 0.2×10^6 to 50×10^6. The test gas is nitrogen. This test was conducted with the 40-inch exit diameter contoured nozzle at a nominal free stream Mach number of 9. Because of the relatively short test times the model wall temperature remained essentially invariant from the initial value of approximately 540°R, thus Tw/To ≈ 0.20 to 0.38. Since the tunnel operates with a constant volume reservoir, the reservoir conditions decay with time. Timewise variations in Reynolds number permit acquisition of data at different Reynolds numbers for the same run. The test model for Tunnel F was a 48 inch, 7 degree half angle cone with eight nose bluntness ratios, R_N/R_B = 0, 0.01, 0.03, 0.05, 0.07, 0.10, 0.15 and 0.37. The model contained 75 coaxial surface thermocouples and 10 surface pressure gages. Nominal model surface finish was 30 microinches and the blunt nose tips were polished before each run. Additional details of Tunnel F and the model instrumentation can be found in Ref. 5.

CHECKS ON GENERALITY OF TRANSITION DATA

In order to utilize boundary layer transition trends obtained in a wind tunnel one has to assume these trends are not uniquely related to the facility being used. The AFFDL Mach 6 wind tunnel had not previously been used for transition investigations and aerodynamic noise measurements had not been made for the tunnel, therefore the basic question of nonuniqueness had to be explored. It has been well established that aerodynamic noise radiating from a turbulent boundary layer on the wall of a supersonic/hypersonic wind tunnel can dominate the transition process on smooth wind tunnel models. In order to compare the influence of aerodynamic noise on transition in the Mach 6 tunnel with other wind tunnels, zero angle of attack, sharp cone transition data was compared with the correlations of Pate[3]. Pate made an extensive study of the relationship between wind tunnel freestream disturbance and boundary layer transition and provided correlations of transition Reynolds number as a function of radiated noise parameters. His results demonstrated a general similarity in the influence of aerodynamic noise on boundary layer transition when the data was correlated in terms of radiated noise parameters. Based upon these studies a method was developed to predict boundary layer transition in wind tunnels; with Mach number, unit Reynolds number and tunnel size as parameters. Fig. 1 indicates Pate's predictions for the end of boundary layer transition on sharp cones in small size wind tunnels. The excellent agreement of these present transition data with the results of Pate indicated that boundary layer transition in the AFFDL tunnel is influenced by aerodynamic noise in a predictable manner, similar to the seventeen wind tunnels considered by Pate. The AEDC Tunnel F was one of the tunnels considered in Pate's study and therefore has demonstrated a similarity with other tunnels.

A comparison of data from two other facilities provided a check on the trends of bluntness effects on transition. These results are shown in Fig. 2. In addition to these present data, wind tunnel results of Muir and Trujillo[6] and shock tunnel results of Stetson and Rushton[7] are included. The data presented in this manner illustrates the rearward displacement of transition in terms of the entropy swallowing. Additional discussions of this manner of presenting blunting data and related blunting characteristics will be included later. The central message to be obtained from this figure is the good agreement of data obtained from different facilities. All three facilities produced the same blunting features and trends, indicating the results were not unique to the facility being used.

Experimenters have usually overlooked or neglected the possibility that the aerodynamic noise radiated from the nozzle boundary layer may not be uniform across the test section. For axisymmetric nozzles there will most likely be some focusing of noise at the tunnel centerline, with some variations radially away from the centerline. When a model is pitched to an angle of attack the nose tip is displaced from the tunnel centerline and may be located in a different noise environment than the zero angle of attack model. It is therefore important to determine if observed transition trends, as a function of angle of attack, are significantly influenced by the location of the model within the test rhombus. A brief investigation of boundary layer transition off the tunnel centerline was made in the AFFDL Mach 6 wind tunnel to assess the problem of nonuniform aerodynamic noise when obtaining transition data at angle of attack. Data was obtained

at two off-centerline stations; at 0.7 and 1.83 inches from the centerline. This was accomplished by inserting a collar on the injection strut to limit the travel of the model support system. The model could not be pitched in the off-centerline position. Data was obtained at zero degrees angle of attack and, by utilizing a bent sting configuration, four degrees angle of attack. Fig. 3 shows the locations of the model in the centerline and off-centerline positions with the four degree bent sting. The tip of the sharp cone was one inch from the nozzle exit. The results obtained with the sharp cone pitched to four degrees angle of attack are shown in Fig. 4. A trend of early transition of the windward side of the model was found for both off-centerline positions. Note from Fig. 3 that when the model was in the 0.7 inch off-centerline location, the model tip was close to the centerline. At this location transition occurred somewhat earlier than the other two locations. Unfortunately details of transition on the leeward side were not clear due to its forward location; however, the end of transition appeared to be unchanged at all three locations. When the sharp tip was replaced with a spherically blunt tip whose radius was ten percent of the base radius (0.2 inches) different transition trends were observed. These results are shown in Fig. 5 with the model at four degrees angle of attack. The onset of transition, for both positions off the centerline, although delayed slightly were not significantly different from the centerline locations. Repeat runs were made of all data and the excellent repeatability demonstrated that the trends shown in Figures 4 and 5 consistently existed. It was demonstrated in this preliminary investigation that varying the location of the model within the test rhombus could vary the transition location up to approximately ten percent. The movement of transition location appeared to be dependent upon model position relative to the tunnel centerline, model attitude, and nose tip bluntness. Additional experiments are required for a good definition of the problem; however, it is believed that variations of aerodynamic noise within the test rhombus will not significantly alter the angle of attack transition trends obtained in this investigation. Fig. 6 compares transition location on the windward ray of a sharp cone with data from a shock tunnel[7], a Ludwieg tube[8], and another wind tunnel[9]. At this time the only guidance as to what the movement of transition with angle of attack should be is the direction of the movement. Both theory (e.g. Moore[10]) and experiment (e.g. Stetson and Rushton[7], Krogmann[8], DiCristina[9]) consistently indicated a rearward movement of the location of transition on the windward ray with angle of attack. The expected magnitude of this rearward displacement is uncertain. All of the facilities shown in Fig. 6 indicated a trend of rearward displacement with angle of attack, with variations in magnitude.

These tests and comparisons provide a reasonable level of confidence that the blunting and angle of attack trends to be presented are general and not uniquely related to a specific facility.

BLUNTNESS EFFECTS

Although the state of the boundary layer on a slender, blunted cone has been under study as an engineering problem for many years, the influence of nose tip bluntness on cone frustum transition remains an area which is poorly understood. The question of why nose tip blunting displaces the onset of transition rearward, and how much rearward displacement should be expected, have never been adequately resolved. From the results of early blunting investigations (e.g. Brinich[11], Moeckel[12]) it was concluded that the rearward displacement of transition was probably due to a reduction in local Reynolds number related to the pressure losses across the bow shock. Stetson and Rushton[7] also concluded that Reynolds number reduction due to blunting was the dominant effect. However, Softley's[13] results, which included a re-interpretation of the data of Stetson and Rushton, obtained local transition Reynolds number twice the sharp cone values. Such a conclusion would suggest that bluntness produced significant changes in the growth of disturbances in a laminar boundary layer.

In addition to changes in local Reynolds number and possible changes in the growth of disturbances in the boundary layer, there is another important consideration involving transition on slender, blunted cones. The Reynolds number for transition may very more than two orders of magnitude along the cone. For example, transition experiments on blunt bodies, such as spherical configurations, have consistently found low transition Reynolds numbers; often less than 500,000 (based on surface distance) and 300 (based on momentum thickness) (e.g. Stetson[14], Anderson[15], Demetriades[16]). Based upon the Mach number independence principle it would be expected that transition in such flows would be essentially independent of free stream Mach number. However, on the frustum of a slender cone, where the entropy layer produced by the blunt tip has been essentially swallowed by the boundary layer, significantly larger transition Reynolds number have been observed, with the magnitude being Mach number dependent, (e.g. Berkowitz, Kyriss and Martellucci[17], Wright and Zoby[18] and Maddalon and Henderson[19]). Local Reynolds numbers, based on surface distance, exceeding 50×10^6 have been obtained. In order to understand and predict transition location on a slender, blunted cone knowledge of the local flow properties is required. One of the problems that currently exists is the inability to assess the uncertainty in local flow calculations and to "sort out" the variations found by using different boundary layer codes. The results of Softley[13] illustrate this problem. Using the data of Ref. 7 he arrived at a conclusion significantly different from that of the original investigation. These differences can be attributed directly to the different techniques used for obtaining local flow properties. Since it may be some time in the future before this problem is adequately resolved, caution should be exercised in drawing conclusions regarding slender, blunted cone transition which are based upon local Reynolds number calculations. In spite of these current shortcomings, a need exists to relate transition location with the influence of the blunt tip in order to establish blunting features and trends. To provide such a

relationship Stetson and Rushton[7] introduced the entropy swallowing length (X_{sw}) as a transition correlation distance. The swallowing distance is defined as the location on the cone frustum where the fluid which has gone through the strong portion of the bow shock has been swallowed by the boundary layer. The local Mach number and flow properties at the edge of the boundary layer at this location are nearly the same as would be obtained on the same cone with a sharp tip (see Fig. 7). For this investigation the method of Rotta[20] was used to obtain swallowing distances. Rotta developed a method to obtain certain boundary layer parameters as a function of a similarity parameter based upon swallowing distance, free stream Reynolds number and nose radius. The curves of Fig. 8 are based upon Rotta's results. This method provided a simple and easy hand calculation technique which is convenient for handling a large amount of experimental data and maintaining a common reference base for comparing results.

Fig. 9 presents local properties on an 8-degree half angle cone with a spherical nose tip radius of 0.04 inches in a $M_\infty = 5.9$ flow. X is the cone frustum distance, with X =0 corresponding to the point of tangency between the tip and cone. These results were obtained with a recently developed boundary layer code[21] based upon integral solutions of the boundary layer equations. Also shown is the swallowing length obtained for this situation by the method of Rotta. The calculated value of X_{sw} corresponds to a location on the cone where the boundary layer code indicated the local Mach number to be 0.97 M_{sharp}. Thus the hand calculated value of X_{sw} is felt to be compatible with these boundary layer code results. For a given cone half angle and free stream Mach number, the swallowing distance varies as $(Re_\infty/FT.)^{1/3}$ and $(R_N)^{4/3}$. Therefore as the nose radius of the cone is systematically increased the swallowing distance also increases. For moderate-to-large nose tip bluntness the entire model is then engulfed with low Mach number, low unit Reynolds number flow. Indicated on Fig. 9 is the region of local flow properties where the maximum rearward displacement of transition location occurred. Thus maximum displacement of transition location on the sphere-cone was found to be associated with essentially blunt-body flow. Even with allowances for possible variations of local properties by utilizing different boundary layer codes, it is believed that this blunt body conclusion should remain valid. This point will be discussed in more detail later. Fig. 10 shows blunting results for four different Mach numbers. The $M_\infty = 3.1$ data was obtained by Rogers[22] in a conventional wind tunnel; the $M_\infty = 5.5$ data is shock tunnel results of Stetson and Rushton[7]; the $M_\infty = 5.9$ results are new data from the AFFDL wind tunnel; and the $M_\infty = 9.3$ data is new data from AEDC's arc-driven Tunnel F facility. The transition lengths for the blunt cones $(X_T)_B$ were normalized by the transition length for the sharp cone $(X_T)_s$[$(X_T)_s$ was different for each facility]. This provides a measure of the rearward displacement of transition on a cone when the sharp tip is replaced with a blunt tip. The abscissa is the transition distance normalized by the swallowing distance (X_{sw}). The swallowing distance for all of these data were based on the results of Rotta (Fig. 8). The right side of the figure ($X_T/X_{sw} > 1$) corresponds to situations where transition occurs on a location on the cone where the entropy layer has been essentially swallowed and the conditions at the outer edge of the boundary layer are nearly the same as would be obtained if the cone had as sharp tip. The left side of the figure (X_T/X_{sw} small) corresponds to locations on the cone just downstream of the tip. The conclusions given below from this type of presentation are not very sensitive to X_{sw}. That is, if a different method of calculating X_{sw} were used which gave different values, the effect would be to shift the data to the right or left and not alter the basic conclusions. Data points shown with an arrow indicate conditions where the entire model had a laminar boundary layer. Transition would then occur at some unknown higher value. The main points to observe in Fig. 10 are as follows:

1. The effect of blunting on transition is very sensitive to free stream Mach number, with large Mach numbers producing large rearward displacement of transition. The reason for this sensitivity with free stream Mach number is believed to be primarily related to the Reynolds number reduction associated with pressure losses across the bow shock. This will become more evident in future discussions.

2. Small bluntness systematically moved the transition location rearward until the maximum displacement was obtained.

3. A blunting transition reversal occurred. That is, additional increases in nose tip radius, or free stream Reynolds number, reduced the value of X_T/X_{sw} and produced a forward movement of transition. This forward movement was very sensitive to both nose radius and Reynolds number. For example, for a given nose radius, a small increase in free stream unit Reynolds number could produce large forward movements of transition. In this situation it was often observed that portions of the cone frustum could be completely laminar while other areas of the model had early transition (this situation may have special significance for persons concerned with the effect of frustum transition on vehicle motion).

4. Maximum rearward displacement of transition occurred in situations where X_T/X_{sw} was small, indicating that the local Mach number was low and the flow was essentially of the blunt-body type (see Fig. 9).

Fig. 11 illustrates the forward movement of transition on a 7-degree half angle cone at a Mach number of about 9.1. At a free stream Reynolds number per foot of 5.4×10^6 the cone had a completely laminar boundary layer. A small increase in free stream Reynolds number caused transition to appear near the cone mid-point at

a local Reynolds number of about 550,000. Further increases in free stream Reynolds number steadily moved the transition location to the sphere-cone tangency point, where the local transition Reynolds number was slightly over 300,000. This forward movement slowed as it progressed through the increasing favorable pressure gradient. These events occurred in a situation where the pressure gradient became increasingly more favorable, yet the transition Reynolds number decreased from 550,000 to nearly 300,000. Further increases in the free stream Reynolds number produced transition in the subsonic region of the tip, with a local transition Reynolds number of about 250,000. The local Reynolds numbers mentioned above were calculated by the finite difference boundary layer code developed by Adams[23] and co-workers. With the exception of the two largest Reynolds number conditions, all of the data of Fig. 11 was obtained during a single run in Tunnel F. These variations in Reynolds number occurred during a 59 millisecond time period while the Mach number varied between 9.1 and 9.0 and the wall temperature remained essentially constant. All of the data shown were obtained along the same ray of the model. This situation, as in most boundary layer transition problems, reflects the result of several competing effects and any explanation of this cone frustum transition behavior at this time would be mostly speculative. The rapid movement of transition from the sphere-cone tangency point to the subsonic region of the tip is not a new observation. This transition pattern was first observed by Stetson[14] over twenty years ago and has been observed by several investigators since that time. It reflects the resistance of the supersonic portion of the nose tip to transition until such time as transition occurs in the subsonic region of the tip.

Fig. 12 was prepared to illustrate the sensitivity of transition location to free stream Mach number. The local Mach number and Reynolds number on a 8-degree half angle cone with a 0.60 inch nose radius was calculated with the boundary layer code of Ref. 23. X is the cone frustum distance, starting at the point of tangency of the tip and cone. Note that the local Mach number was low for both cases and relatively insensitive to free stream Mach number. As far as local Mach number is concerned the two flows were quite similar. The surface pressure distributions (not shown) differ somewhat, due to the fact that the region of overexpansion and subsequent recompression are Mach number dependent. Significant differences were found in the local Reynolds number. These differences are related to the fact that the total pressure losses across the bow shock increased with Mach number. The experimentally observed transition location for these two free stream Mach number situations are indicated and it can be seen that even though the transition locations differ considerably, the local Reynolds number for transition was essentially the same for both cases. These results indicated that the difference in transition location for the two cases shown can be accounted for by the Reynolds number reduction associated with the total pressure losses across the bow shock.

Fig. 13 provides additional information to demonstrate the relationship between transition location and Reynolds number reduction. The trend of maximum transition displacement with free stream Mach number clearly follows the trend of Reynolds number reduction. These results, as well as those of previous figures, provide convincing evidence that the maximum rearward displacement of transition is directly related to the Reynolds number reduction. For supersonic and moderately hypersonic flows it should be possible to predict the maximum rearward displacement of transition on a slender cone due to blunting with reasonable confidence as long as other effects, such as ablation, roughness, and angle of attack do not play a dominant role.

Fig. 14 is shown partly to demonstrate the problem of calculating local Reynolds number and partly to illustrate the different flow situations found on a blunted, slender cone. The local Reynolds number for these present $M_\infty = 5.9$ data were obtained by using the unit Reynolds number profile shown in Fig. 8 and assuming that the relationship between Rotta's swallowing distance and this profile was the same for all of the data. The results of Softley[13], with local transition Reynolds numbers of twice the sharp cone value, are shown for comparison. Since Softley's results had the entropy layer being swallowed much more rapidly than these present calculations, the local Reynolds numbers he calculated for transition were significantly larger in the small-to-medium bluntness regime. Since it is not possible to adequately assess at this time the accuracy of flow field calculations of this type, the "correct" trend for a local Reynolds number plot such as this is not known. The fact that the maximum Reynolds number shown for Softley's results coincide with the large increase in Re_{X_T} for these present data is believed to be fortuitous since the swallowing distances for the two sets of data are not compatible. The data on the left side of the figure, which should be relatively insensitive to the particular method used for calculating local Reynolds number, indicates frustum transition Reynolds number become small, of the same order as those found on nose tips, when transition occurs early on the cone frustum. It appears that for cases of small bluntness, local transition Reynolds number greater than those obtained on a sharp cone are possible; however, attaching a specific number seems to have little significance at this time. Martellucci[24] also calculated local Reynolds numbers for the data of Ref. 7, using a finite-difference boundary layer code, and obtained local transition Reynolds numbers, for the case of small bluntness, somewhat larger than the sharp cone values.

ANGLE OF ATTACK

Although transition trends on a sharp cone at angle of attack may defy one's intuition, there seems to be general agreement regarding the expected movement of transition. Theory and experiment both indicate a rearward movement of transition on the windward ray and a forward movement on the leeward ray. Moore's[10] results

show that the boundary layer profiles assume a more stable shape on the windward side and a more unstable shape on the leeward side. Hot wire experiments of Kendall[25] at $M_\infty = 4.5$, which measured the boundary layer fluctuation spectra on the windward and leeward rays of a 4-degree half angle sharp cone, qualitatively confirm these theoretical predictions. References 7-9 provide additional examples of confirmation of these trends.

Fig. 15 illustrates the local Reynolds numbers associated with the transition movements on the windward and leeward rays of a sharp, 8-degree half angle cone in a $M_\infty = 5.9$ flow. The local transition Reynolds number increased on the wind ray and decreased on the leeward ray.

Fig. 16 illustrates the transition movement on the windward and leeward rays of an 8-degree half angle cone at $M_\infty = 5.9$. The transition distance (X_T) is normalized by the transition distance on the sharp cone at $\alpha = 0^o$ [$(X_{T_s})_{\alpha=0}$ varies with unit Reynolds number]. It was planned to test all of the blunt configurations at the same free stream unit Reynolds number; however, for the 15% blunt tip, transition moved off the end of the model at $\alpha = 2^o$. Therefore this configuration was tested at a slightly larger Reynolds number. The sharp cone transition trends were consistent with expected results, as noted earlier. The blunt configurations; however, have trends which are somewhat different from those of Ref. 7. These differences relate to the windward ray at small angles of attack. Ref. 7 had the maximum rearward displacement at $\alpha = 0^o$ and a forward movement with angle of attack. The present data consistently had a rearward movement initially, as for the sharp cone, and then a forward movement at larger angles of attack. The reason for these differences is not known. Intuitively it would seem reasonable that the blunt cone boundary layer profiles might assume a more stable shape with angle of attack, analogous to the sharp cone, and therefore cause transition to move rearward on the windward ray. Transition would not continue to move rearward, as for the sharp cone, since the effect of bluntness diminishes with angle of attack. It would be expected that the curve would turn and approach the sharp cone curve. At some large angle of attack all of the curves should merge into a single curve. Variations of tunnel aerodynamic noise, as discussed earlier, may have a small influence on these data; however, it is not believed to be an effect capable of altering the major trends shown in Fig. 16.

The data obtained with the 30% blunt nose tip is presented separately (Fig. 17) due to the nature of the results. Initial experiments were conducted at $Re_\infty/Ft. = 19.4 \times 10^6$, as were the other blunt configurations of Fig. 16. The windward ray was completely laminar at all angles tested. Increasing the free stream unit Reynolds number produced a condition where the laminar boundary layer previously had been observed to be in a rather delicate balance; one in which transition could be easily initiated (in Fig. 10 this corresponds to situations where X_T/X_{SW} is in the range of 0.02 to 0.03 and is also illustrated in Fig. 11 for the Tunnel F data). The $\alpha = 0^o$ data shown in Fig. 17 is the same data shown in Fig. 10. A small change in Reynolds number or repeated experiments at a given Reynolds number (open circles) produced a wide range in transition locations. A unit Reynolds number of 28 million was selected for the angle of attack tests in order to keep transition from moving off the model on the windward ray. The results are shown with the solid circles. The windward ray transition locations seemed to have two preferred locations - a large displacement and a short displacement. It can be seen from this figure that several transition trends are possible at this condition and it was not possible to predict where transition would occur.

BICONIC CONFIGURATIONS

A sample of the transition data on the biconic configuration with a sharp tip is shown in Fig. 18. The local values of Mach number, Reynolds number and heat transfer coefficient predictions were obtained from the boundary layer code of Ref. 21. The local Reynolds number at the transition location was about 6 million. Similarly, transition Reynolds numbers on the sharp, 8-degree cone were nearly 6 million for this freestream condition. Fig. 19 presents similar results for the blunt biconic configuration. The local transition Reynolds number for this situation was about 3 million, which was comparable to local transition Reynolds numbers on the 8-degree cone with moderate blunting (see Fig. 14).

Fig. 20 indicates the transition locations on the windward and leeward rays of the sharp and blunt biconic configurations. The data is normalized with the transition location on the sharp biconic at $\alpha = 0^o$, in a manner similar to that used for the 8-degree cone data. It was found that the junction between the two cones often acted as a boundary layer trip, in an unpredictable manner. In respect to this apparent tripping of the boundary layer it should be noted that special care was taken in the construction of the model to avoid surface irregularities at this junction. The 14-degree nose piece was constructed with a slight rearward facing step at the junction; then after the model was assembled it was polished to provide a smooth connection. The upper windward curve for the blunt biconic corresponds to transition on the aft cone. The lower windward data corresponds to transition near the junction of the two cones. For the sharp biconic the upper curve also relates to transition on the aft cone. At $\alpha=4^o$ transition occurred on the windward ray at the junction of the cones for both tests. At $\alpha=8^o$ one test produced transition on the aft cone and a duplicate run had transition on the fore cone.

The biconic configurations utilized in this investigation did not produce any significant delays in boundary layer transition and, in fact, often promoted an early transition.

CONCLUSIONS

Following are the major conclusions obtained from this investigation:

1. Comparison of these present boundary layer

transition data with data from other facilities and transition experiments off the tunnel centerline indicated the blunting and angle of attack trends obtained were general and not uniquely related to the facility used.

2. The rearward displacement of transition due to tip bluntness was found to be quite sensitive to free stream Mach number as well as to bluntness. At M_∞ = 9.3 transition could be displaced rearward as much as nine times the transition length for a sharp cone.

3. Small bluntness systematically moved the transition location rearward until the maximum displacement was obtained.

4. A blunting transition reversal occurred. That is, additional increases in nose tip radius, or free stream Reynolds number, produced a forward movement of transition.

5. The forward movement of transition took place rapidly, with small changes in Reynolds number or nose radius. Asymmetric transition fronts at $\alpha = 0^0$ were common for this situation.

6. The maximum rearward displacement of transition occurred under situations of low local Mach number flow.

7. The trend of maximum transition displacement with free stream Mach number followed the trend of Reynold number reduction. Reynolds number reduction is believed to be the dominant effect associated with the rearward displacement of transition.

8. Transition correlations based on local Reynolds number should be used cautiously, since it is not possible, at this time, to assess the accuracy of the Reynolds number calculations.

9. Transition locations were sensitive to small changes in angle of attack. Both the sharp and blunt tips produced a rearward movement of transition on the windward ray at small angles of attack.

10. The 30% blunt cone produced several transition trends and it was not possible to predict where transition would occur.

11. The biconic configurations investigated did not produce any significant delays in boundary layer transition (compared to a cone) and, in fact, often promoted an earlier transition.

REFERENCES

1. Mack, L.M., "Transition and Laminar Instability," JPL publication 77-15, May 1977 (NASA-CP-153203)

2. Wilcox, D.C. and Traci, R.M., "A Complete Model of Turbulence," AIAA paper No. 75-351, San Diego, California, 1976.

3. Pate, S.R., "Dominance of Radiated Aerodynamic Noise on Boundary-Layer Transition in Supersonic-Hypersonic Wind Tunnels, Theory and Application," AEDC-TR-77-107, March 1978.

4. Fiore, A.W. and Law, C.H., "Aerodynamic Calibration of the Aerospace Research Laboratories M=6 High Reynolds Number Facility," ARL-TR-75-0028, Feb. 1975.

5. Test Facilities Handbook (Tenth Edition), "von Karman Gas Dynamics Facility, Vol. 3," Arnold Engineering Development Center, May 1974.

6. Muir, J.F. and Trujillo, A.A., "Effects of Nose Bluntness and Free Stream Unit Reynolds Number on Slender Cone Transition at Hypersonic Speeds," Proceeding of the Boundary Layer Transition Workshop, Vol. III, 20 Dec. 1971, Aerospace Report No. TOR-0172 (S2816-16) -5.

7. Stetson, K.F. and Rushton, G.H., "Shock Tunnel Investigation of Boundary Layer Transition at M=5.5," AIAA Journal, Vol. 5, pp. 899-906 (May 1967).

8. Krogmann, P. "An Experimental Study of Boundary-Layer Transition on a Slender Cone at Mach 5, "AGARD Symposium on Laminar-Turbulent Transition, Technical University of Denmark, Copenhagen, Denmark, 2-4 May 1977

9. DiCristina, V. "Three-Dimensional Laminar Boundary-Layer Transition on a Sharp 8^0 Cone at Mach 10," AIAA Journal, Vol. 8, pp. 852-856 (May 1970).

10. Moore, F.K., "Laminar Boundary Layer on a Circular Cone in Supersonic Flow at Small Angle of Attack," NACA TN 2521 (Oct 1951).

11. Brinich, P.F., "Effect of Leading-Edge Geometry on Boundary-Layer Transition at Mach 3.1," NACA TN 3659 (March 1956).

12. Moeckel, W.E., "Some Effects of Bluntness on Boundary-Layer Transition and Heat Transfer at Supersonic Speeds," NACA Rept. 1312 (1957).

13. Softley, E.J., "Boundary Layer Transition on Hypersonic Blunt, Slender Cones," AIAA paper No. 69-705 (June 1969).

14. Stetson, K.F., "Boundary-Layer Transition on Blunt Bodies with Highly Cooled Boundary Layers," J.A.S. Vol. 27, pp. 81-91 (Feb.1960)

15. Anderson, A.D., "Interim Report, Passive Nosetip Technology (PANT) Program, Vol. X, Appendix, Boundary Layer Transition on Nosetips with Rough Surfaces, SAMSO-TR-74-86 (Jan. 1975).

16. Demetriades, A., "Nosetip Transition Experimentation Program, Final Report, Vol. II," SAMSO-TR-76-120 (July 1977).

17. Berkowitz, A.M., Kyriss, C.L. and Martellucci, A., "Boundary Layer Transition Flight Test Observations," AIAA paper No. 77-125 (Jan. 1977).

18. Wright, R.L., and Zoby, E.V., "Flight Boundary Layer Transition Measurements on a Slender Cone at Mach 20", AIAA paper No. 77-719 (June 1977).

19. Maddalon, D.V., and Henderson, A., Jr., "Boundary Layer Transition at Hypersonic Mach Numbers," AIAA paper No. 67-130 (Jan. 1967).

20. Rotta, N.R., "Effects of Nose Bluntness on the Boundary Layer Characteristics of Conical Bodies at Hypersonic Speeds," NYU-AA-66-66 (Nov. 1966).

21. Hecht, A.M. and Nestler, D.E., "A Three-Dimensional Boundary-Layer Computer Program for Sphere-Cone Type Reentry Vehicles, Vol. 1, Engineering Analysis and Code Description," AFFDL-TR-78-67 (June 1978).

22. Rogers, R.H., "Boundary Layer Development in Supersonic Shear Flow," Boundary Layer Research Meeting of the AGARD Fluid Dynamics Panel, London, England, AGARD Rept. 269 (April 25-29, 1960).

23. Adams, J.C., Jr., Martindale, W.R., Mayne, A.W., Jr., and Marchand, E.O., "Real-Gas Scale Effects on Shuttle Orbiter Laminar Boundary-Layer Parameters," Journal of Spacecraft and Rockets, Vol. 14, pp 273-279 (May 1977).

24. Martellucci, A., private communication.

25. Kendall, J.M., unpublished paper (1971).

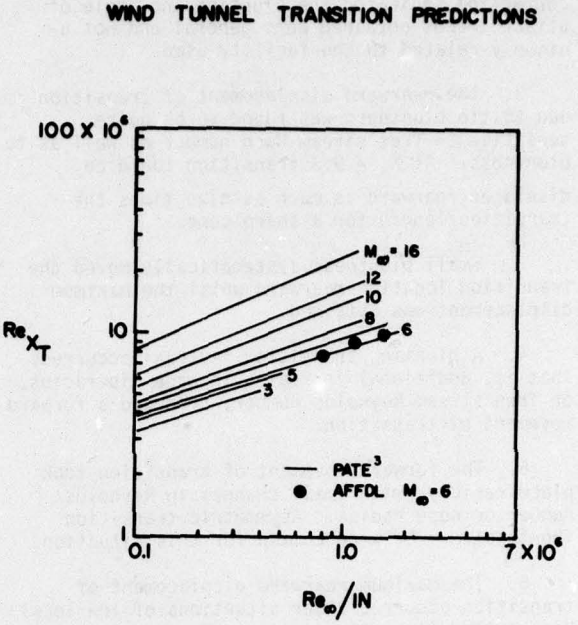

Figure 1 Effect of Mach number and unit Reynolds number on sharp cone transition for small size wind tunnels(Re_{X_T} is the end of transition) X_T (from Pate[3])

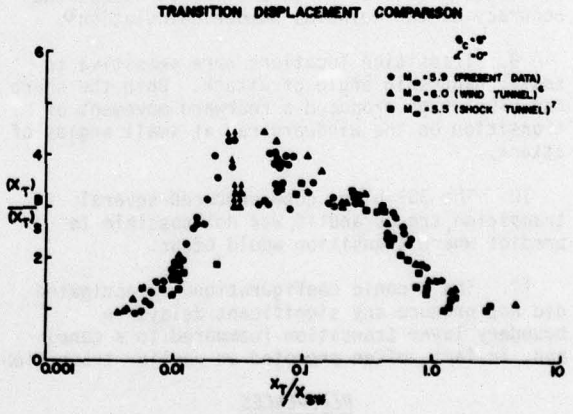

Figure 2 A comparison of bluntness effects in three facilities

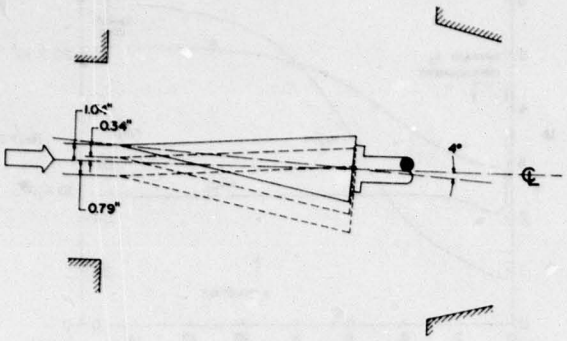

Figure 3 Sharp cone positions with a 4-degree bent sting

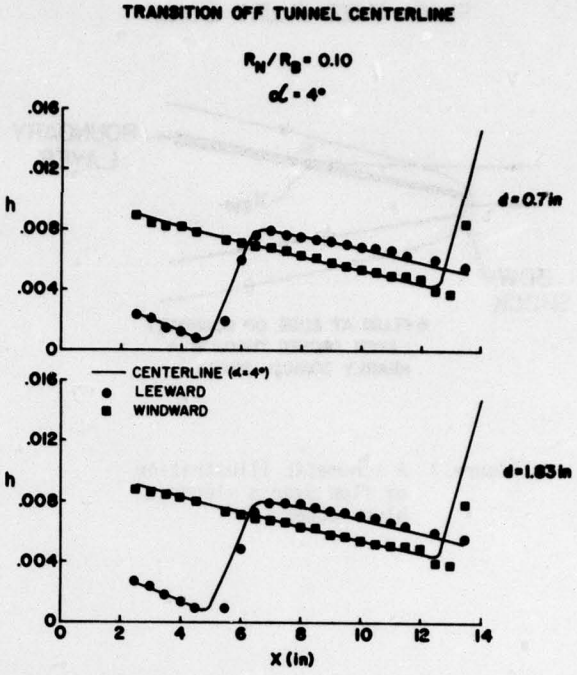

Figure 5 Heat transfer coefficient distributions for the 10% blunt cone with a 4-degree bent sting at three positions

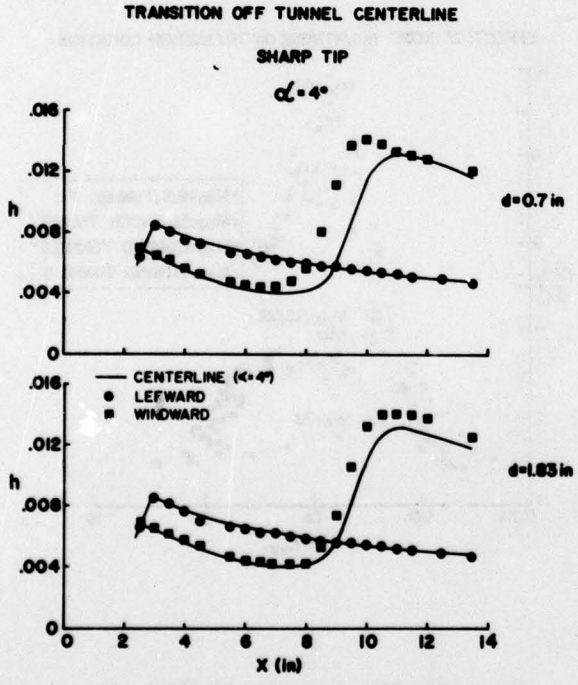

Figure 4 Heat transfer coefficient distributions for the sharp cone with a 4-degree bent sting at three positions.

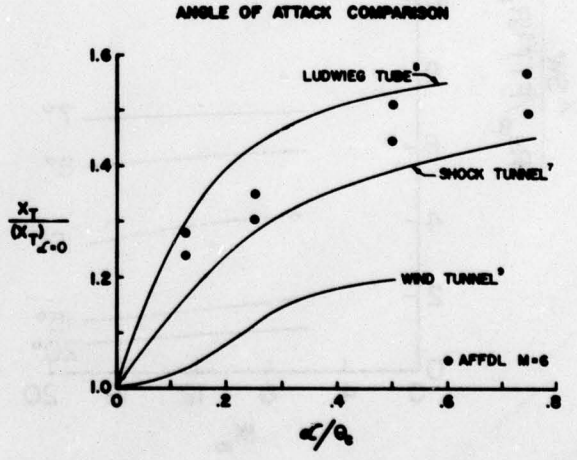

Figure 6 A comparison of the movement of transition on the windward ray of a sharp cone

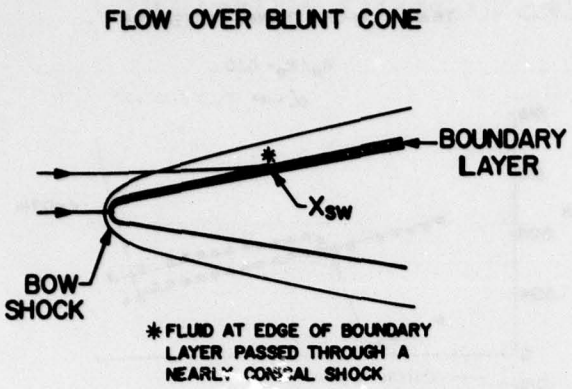

Figure 7 A schematic illustration of flow over a slender, blunt cone.

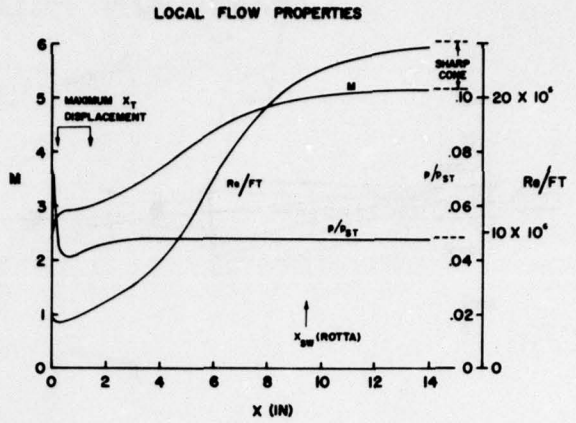

Figure 9 Calculations of local flow properties on a 8-degree half angle cone with 2% bluntness (R_N=0.04 inches) at at M_∞ = 5.9

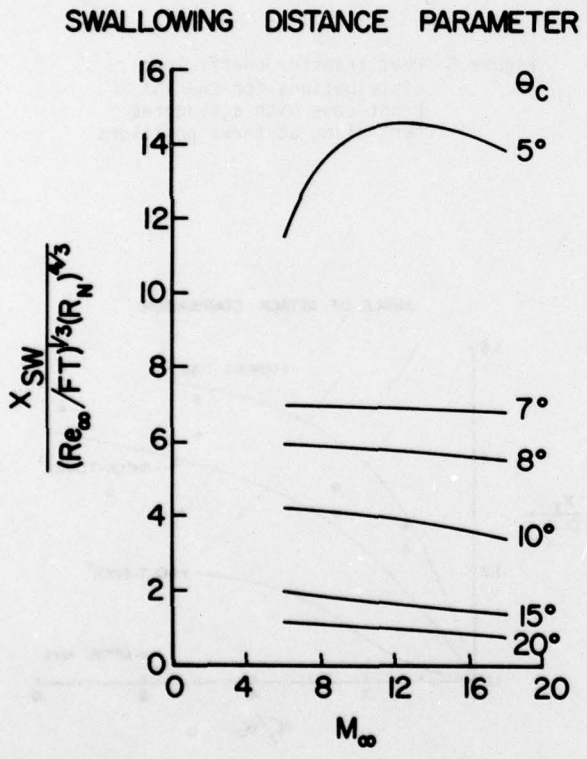

Figure 8 Swallowing distance parameter

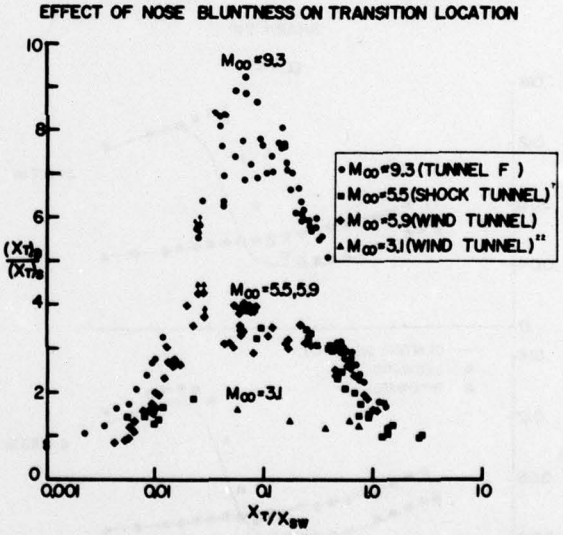

Figure 10 Effect of nose bluntness on transition location.

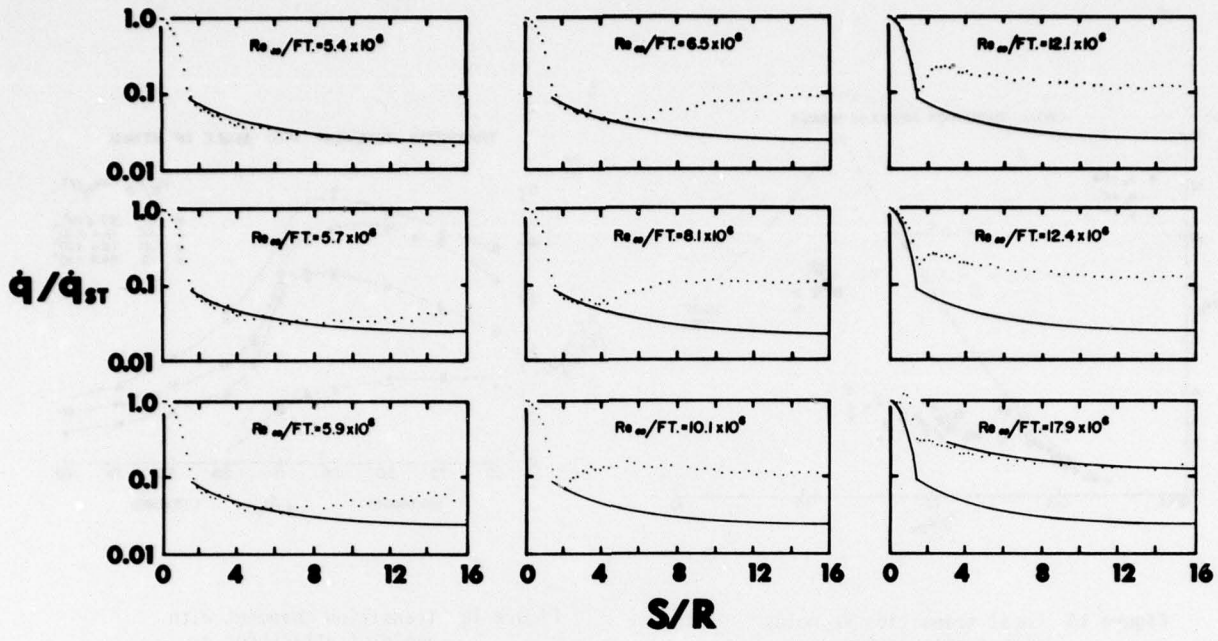

Figure 11 Transition movement from cone frustum to nose tip on a 7-degree half angle cone at $M_\infty \simeq 9.1$

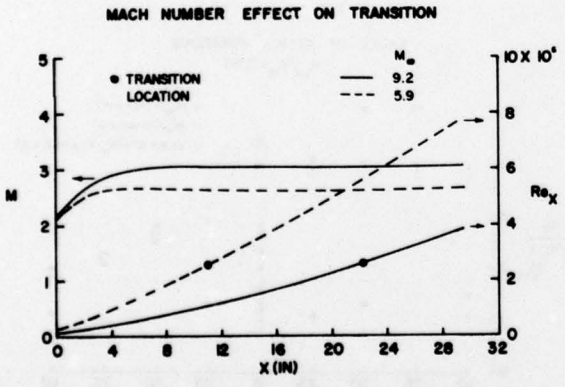

Figure 12 Transition location and local Mach number and Reynolds number on a 8-degree half angle cone with a 0.60 inch nose radius at M_∞=5.9 and 9.2.

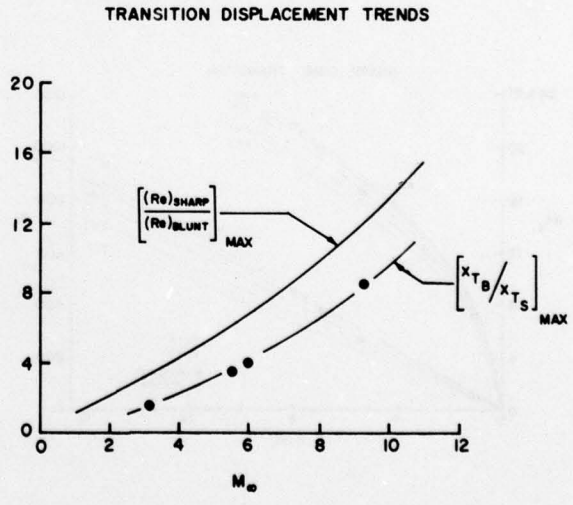

Figure 13 Transition displacement trend with Mach number

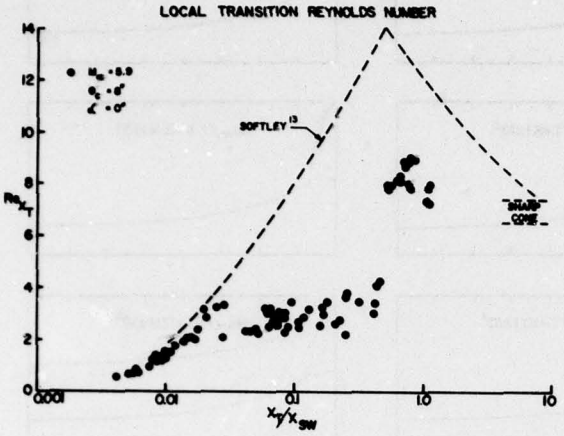

Figure 14 Local transition Reynolds number calculations

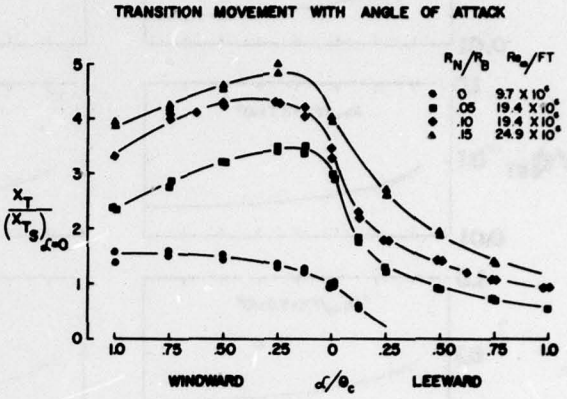

Figure 16 Transition movement with angle of attack for a 8-degree half angle cone at M_∞=5.9

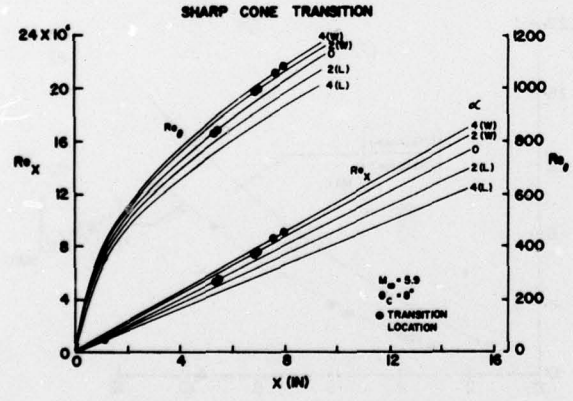

Figure 15 Local Reynolds number calculations on a sharp cone at angle of attack

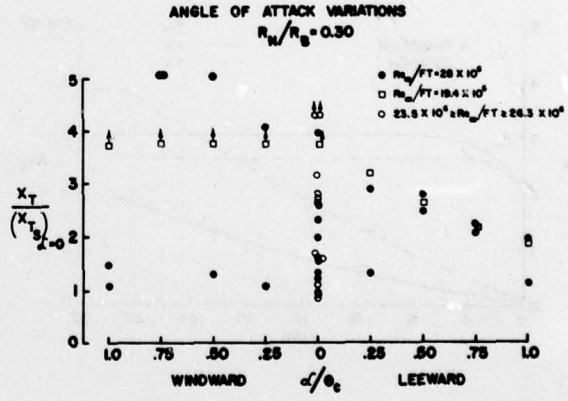

Figure 17 Transition movement with angle of attack for a 8-degree half angle cone with 30% bluntness at M_∞=5.9

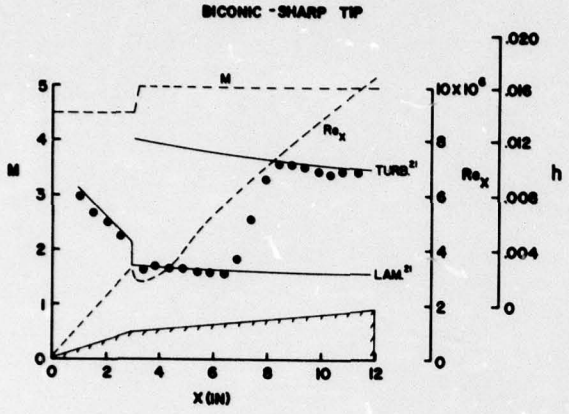

Figure 18 Heat transfer coefficient distribution and local flow calculations on a biconic configuration with a sharp tip and M_∞=5.9

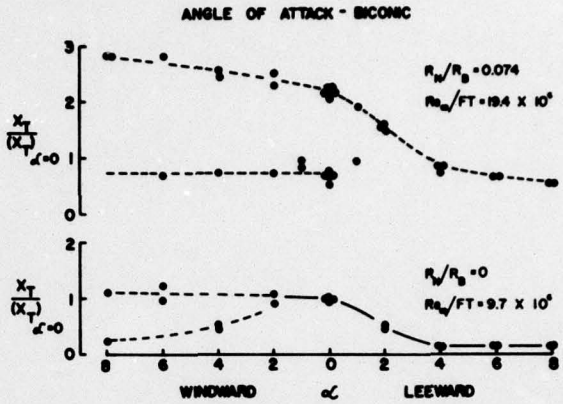

Figure 20 Transition movement with angle of attack for the biconic configurations at M_∞=5.9

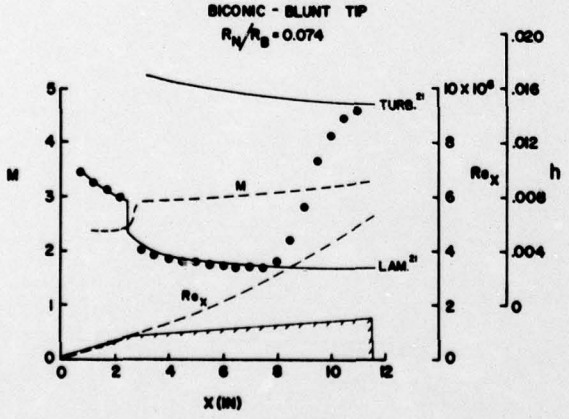

Figure 19 Heat transfer coefficient distribution and local flow calculations on a biconic configuration with a blunt tip at M_∞=5.9